ARMA 21–2121

Influence of the pore fluid type on the observation of induced seismicity

Makhnenko, R.Y., and Bondarenko, N.B.

Department of Civil and Environmental Engineering, University of Illinois at Urbana-Champaign, Urbana, IL, USA

ABSTRACT: Injection of fluids in the subsurface can induce seismicity and possibly lead to rock failure. Earthquake nucleation could be triggered by pore fluid diffusion or changes in pore fluid composition. Thus, microcracking processes before the formation of macrofracture in fluid-saturated rock are of major importance. Plane strain compression experiments were performed on dry, oil- and water-saturated Berea sandstone under different boundary conditions. The deformation of the material was measured and the acoustic emission (AE) activity was recorded. Onset of inelastic response coincided with an increase in AE rate. However, released energy and onset of inelastic behavior were influenced by the pore fluid. Presence of oil in the pores did not affect the AE behavior. Earlier onset of recorded AE activity in water-saturated compared to dry and oil-filled specimens is explained by stress corrosion cracking, which resulted in microcracking at relatively low deviatoric stresses. In contrast to the yield envelope, the failure envelope was not affected by type of pore fluid. We suggest performing laboratory experiments that closely replicate the in-situ conditions in terms of applied external stresses, pore pressures, temperatures, and type pore fluids to properly characterize the potential of inducing seismic activity in rock during underground storage.

1. INTRODUCTION

Injection of fluids into the subsurface reduces the effective stress and can cause microcracking or slip of existing fractures, which lead to induced seismicity (Ellsworth, 2013). Geothermal energy systems, conventional and unconventional oil and gas recovery, and CO_2 storage technologies all involve fluid withdrawal and/or injection, thereby providing the potential to induce seismic events (National Research Council, 2012). An application of new and innovative laboratory methods allows a better understanding of the complex, coupled processes in the subsurface energy extraction applications and corresponding risks of fluid-induced seismicity (Benson et al., 2020). Acoustic emission (AE) monitoring techniques used in the laboratory are similar to microseismicity monitoring applied at field-scale (Lei and Ma, 2014). Generally, AE is a process of elastic wave emission associated with microcrack growth during inelastic deformation; features of the AE represent the process of fault nucleation and allows studying seismicity at laboratory scale (Lockner, 1993).

The effect of pore fluid on AE behavior in rock is reported since Byerlee and Lockner, 1977. Water injection into initially dry rock close to the peak stress has been shown to initiate the fracture processes (Stanchits et al., 2011). Uniaxial compression tests conducted by Tarokh et al. (2020) on dry specimens of the Berea sandstone before and after injection of liquid CO_2 do not show a significant effect of CO_2 treatment on microcracking activity. However, pore fluid presence is known to affect rock properties and mechanical behavior (Rice, 1975; Detournay and Cheng, 1993). The presence of aqueous pore fluids may also influence the inelastic rock deformation due to the chemical effect that allows cracks to propagate even at low stresses through stress corrosion (Atkinson and Meredith, 1987). Therefore, it is expected that the microcracking processes could differ for dry and fluid-saturated rock. Moreover, AE behavior can also depend on the type of the pore fluid. Results of compression tests conducted by Zang et al., 1996 on Flechtingen sandstone and Smirnov et al., 2020 on Buffalo sandstones demonstrate promotion of AE activity in wet rock comparing to the dry one. Mayr et al., 2011 showed that acoustic emission events before formation of macroscopic fracture are triggered by the migration of a critical pore pressure; however, formation of a sample-scale fracture was more likely controlled by the localization of damage. Experiments conducted by Li et al., 2016 demonstrated that AE activity for fully water-saturated specimen of sandstone from Sichuan Basin, China is only 5% of that in the partially saturated specimen. In addition, the authors noticed that for the partially saturated rock, AE activity initiates earlier comparing to the fully saturated one. Sobolev et al., 2010 noticed that water is capable of initiating the fracture process by chemical effect without increasing the pore

pressure. In contrast to the effect of water on AE behavior, there is much less information about the effect of other types of pore fluids and their influence on the corresponding fracturing process.

In this study, Berea sandstone is tested in plane strain compression at four boundary conditions: dry, water-saturated drained, water-saturated undrained, and oil-saturated unjacketed. Localization of damage is monitored by recording AE. The differences between the microcracking activity recorded in dry and oil-saturated tests comparing to the water-saturated tests are discussed.

2. EXPERIMENTAL METHODS

2.1. Compression of fluid-saturated rock

Laboratory tests were conducted using the University of Minnesota Plane-Strain Apparatus (Labuz et al., 1996). The prismatic specimen (100 mm width, 87 mm height, and 44 mm thickness) is sealed with a polyurethane jacket and subjected to loading. The major principal stress σ_1 (vertical) is applied with an axial piston, and load is measured with a load cell. The intermediate stress σ_2 is created by a passive restraint - a thick-wall steel cylinder (biaxial frame) and can be evaluated from the biaxial frame deformation (Makhnenko and Labuz, 2014). The minimum principal stress σ_3 is applied with the hydraulic oil, which fills the apparatus. Normal strains ε_1 and ε_3 aligned with the principal stress directions are obtained from the displacements measured by LVDTs in axial and lateral direction, corrected for the system compliance.

A back pressure saturation technique is utilized to achieve full water saturation. The first stage consists of flushing the water through the specimen until the injected fluid volume is equal to the collected one. In the next stage, the outlet valve is closed, and pore (back) pressure is gradually increased with preserving effective mean stress constant. The specimen is assumed to be fully saturated when the Skempton's *B* coefficient reaches a constant value (Makhnenko and Labuz, 2016).

Dry experiments are conducted on oven-dry specimens covered with a jacket to prevent oil penetration. Water saturated drained condition is achieved by preserving a constant pressure in the back pressure controller connected to the fully saturated specimen. Closing the valve in the pressure line between controller and specimen allows imposing undrained boundary condition, where the pore pressure is monitored by a pressure transducer placed between the valve and the specimen. In oil-saturated unjacketed condition, the pore pressure preserved equal to the minimum principal stress σ_3. This condition is achieved by not covering the specimen with polyurethane and allowing hydraulic oil to penetrate and saturate the initially dry specimen.

2.2. Acoustic emission methods

AE is monitored by eight sensors (Physical Acoustics model S9225, frequency response from 0.1 to 1.2 MHz). AE signals are preamplified (Physical Acoustics model S1220C) with a 40 dB gain and filtered with 0.1-1.2 MHz band-pass filter. The sampling rate is 20 MHz with 0.2 ms for each acquisition's time length and 0.1 ms pretrigger. Recorded AE was interpreted in terms of total number of events and actual waveforms analysis (Makhnenko et al., 2020).

AE activity correlates with number of generated microcracks, and this tendency can be evaluated on the basis of the rate process theory (Ohtsu et al., 1993). A probability density function *f(V)* of AE occurrence is defined to relate the AE activity to material damage during the application of stress:

$$f(V)dV = \frac{dN}{N_0}, \tag{1}$$

where V is a ratio between shear stress $\tau = (\sigma_1 - \sigma_3)/2$ corresponding to the N^{th} event number and the shear stress at failure $[\tau]$: $V = \tau/[\tau]$, and N_0 is the total number of acoustic emission events up to failure. The function *f(V)* describes the rate of microcracking within the material during an increment of the applied stress dV and satisfies the condition that the total area under its curve versus V is 1:

$$\int_0^1 f(V)dV = 1. \tag{2}$$

The relationship between V and N can be established from the experimental data and typically has the form (Dai and Labuz, 1997):

$$V = aN + c \cdot \ln(1 + qN), \tag{3}$$

where a, c, and q are the fitting parameters found from the experimental data. From Eqs. (1) and (3) the following relationship can be written for *f(V)*:

$$f(V) = \frac{1}{N_0}\left(\frac{1+qN}{a+cq+aqN}\right). \tag{4}$$

This function can be evaluated from the recorded AE and plotted versus the stress ratio. A larger value of the probability density function for a given V indicates a greater AE rate and more stress-induced microcracks. Results of this analysis for dry, water-saturated, and oil-saturated tests are shown in the next section.

The relative energy of an AE event can be related to a root-mean-square value (*RMS*) that can be evaluated by taking the actual voltage *g(t)* at each point along the AE waveform *g(t)* and averaging the square of *g(t)* over time period *T:*

$$RMS = \sqrt{\frac{1}{T}\int_0^T |g(t)|^2 \, dt}. \qquad (5)$$

Signals recorded with AE sensors are band limited, therefore frequency dependence was not studied. The study is focused on the analysis of AE signals to estimate relative emitted energy. A signal recorded at only one sensor should not be used to estimate released energy due to the geometric attenuation of the signal. However, for a large number of sensors with sufficient spacing, an average *RMS* value from all the sensors will be representative of the released energy.

3. EXPERIMENTAL RESULTS

Berea sandstone was tested at dry, oil-saturated unjacketed, and water-saturated drained and undrained conditions. Recorded shear stress- shear strain curves are shown for dry (Figure 1a), unjacketed (Figure 1b), drained (Figure 1c), and undrained (Figure 1d) tests, where shear strain is $\gamma = \varepsilon_1 - \varepsilon_3$. The continuous AE activity is shown to match the onset of inelasticity determined from volume strain – shear strain diagram for each test (Makhnenko et al., 2020). Recorded AE data is analyzed in terms of cumulative number of events. Since the load corresponding to each event is known, the stress ratio V can be calculated. Figure 2 illustrates the curves of the event number N versus stress ratio V for dry (Figure 2a), unjacketed (Figure 2b), drained (Figure 2c), and undrained (Figure 2d) sandstone specimens compressed under plane strain condition up to peak load. Generally, the AE activity increases with an increase of the load. Furthermore, the fitting parameters a, c, and q from Eq. (3) can be evaluated from a nonlinear curve fitting regression to express probability density function $f(V)$.

Comparison of the probability density functions for the dry, unjacketed, drained, and undrained test is shown in Figure 3. Drained and undrained specimens with water filling the pore space exhibit similar behavior up to 75% of peak stress. Acoustic emission initiates at relatively small stress ratio (about 30%) and has approximately constant activity from the onset of inelasticity (yield) up to failure. This behavior is similar to the one of medium-strength rock specimens with defects (Dai and Labuz,

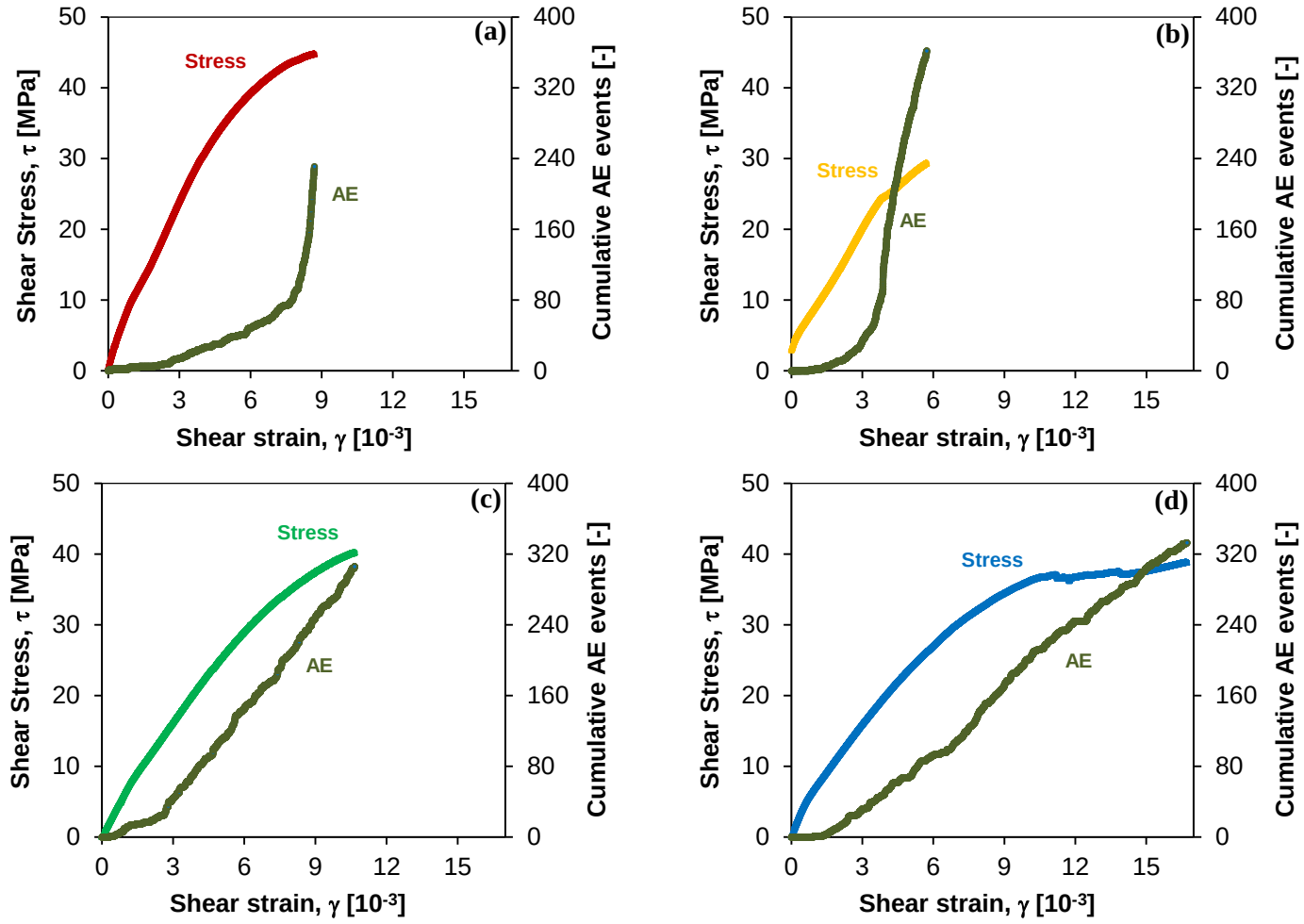

Fig. 1. Stress-strain curves and cumulative number of AE events for (a) dry, (b) unjacketed oil-saturated, (c) drained water-saturated, and (d) undrained water-saturated plane strain compression experiments.

1997). In contrast to this behavior, dry and oil-saturated unjacketed specimens demonstrate that most of the AE events have been initiated at significantly higher stress ratios (95% for dry and 85% for unjacketed specimens), similar to the one observed by Dai and Labuz (1997) for dry medium strength rock (sandstone).

Analysis of actual AE waveforms was conducted for dry and water-saturated drained plane strain compression experiments (Figure 4). At stress ratios below 80%, the energy released by AE in the saturated test was higher than the one for the dry case. However, closer to the peak stress the total *RMS* for dry test increased significantly and became two times larger comparing to the water-saturated specimen. Signals recorded in the water-saturated test qualitatively are similar to a swarm-like seismicity where all events have similar magnitudes and rapid changes in released energy are absent (Fischer et al., 2014). At the same time, signals from the dry test are more similar to the process of the earthquake preparation (Scholz, 2019). The energy released by the creation of individual microcracks is relatively small; however, the transition of fracturing process from microcrack-scale to sample-scale fracture is accompanied by the significant increase of released energy near to the peak stress level.

4. DISCUSSION

Peak strength and AE data for dry, unjacketed, drained, and undrained tests (two of each kind) are are used to construct Mohr-Coulomb failure and yield envelopes (Figure 5), where $s' = (\sigma_1+\sigma_3)/2 - p^f$ is the effective average stress and p^f is the pore pressure. The common intercept on x-axis (in-plane tensile strength) is assumed for the failure and yield envelopes. While a common linear failure surface can be constructed for all the tests, the yield points appear to be significantly different for drained and undrained loading comparing to dry and unjacketed tests. Basically, two yield surfaces can be constructed and the onset of inelasticity for water-saturated rock is lowered comparing to dry and oil-saturated specimens. The observed difference in AE behavior may be caused by the chemo-mechanical weakening effect of water, which is not observed for dry and oil-saturated unjacketed specimens. In the case of Berea sandstone, the significant weakening effect most probably was caused not by the dissolution of some of the rock minerals (the rock matrix consists of 90% quartz, 8% feldspar, and less than 1% calcite), but the creation of microcracks due to the stress corrosion.

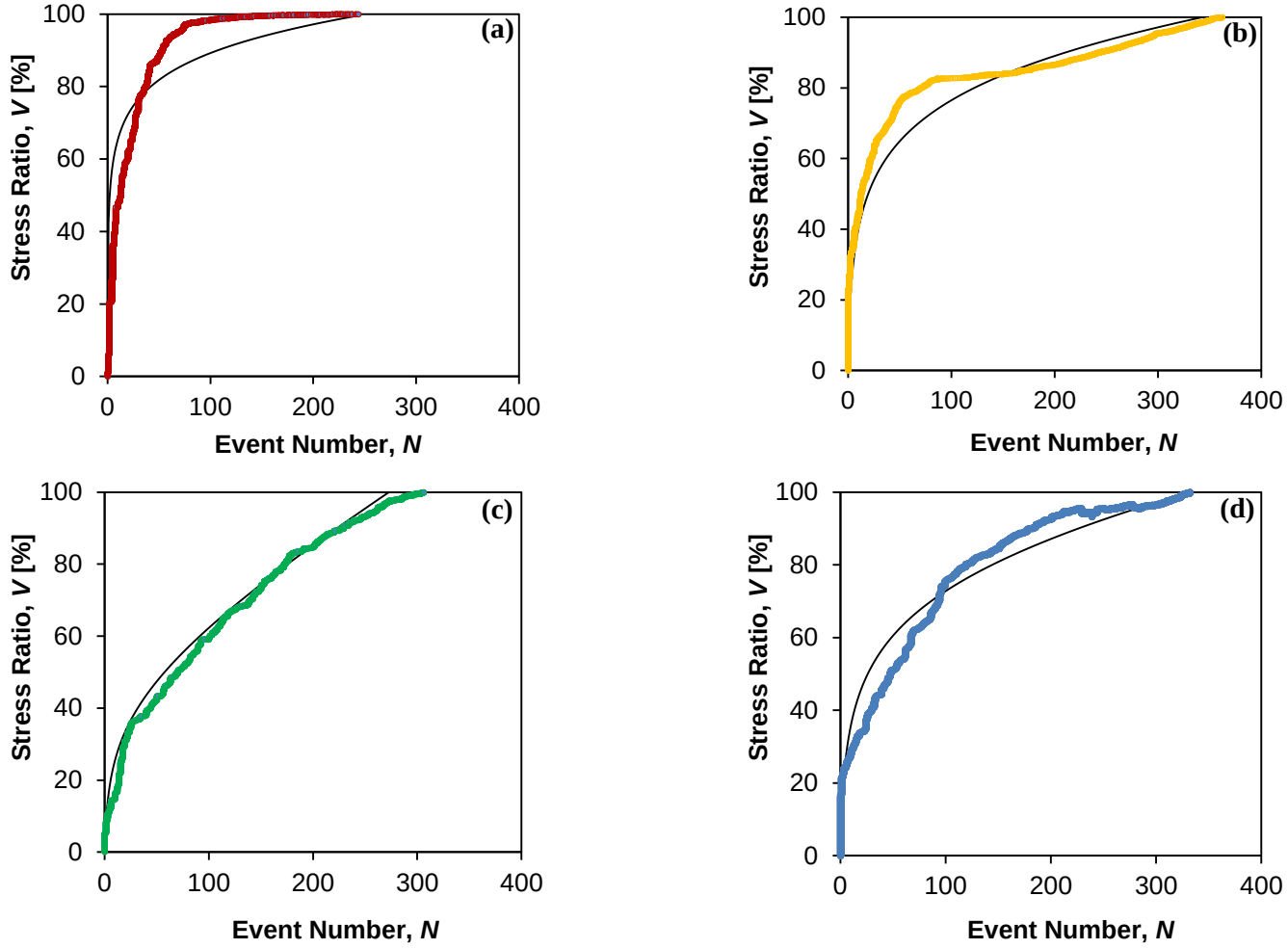

Fig. 2. Stress ratio versus event number and fitted curves (black) for Eq. (3) for (a) dry, (b) unjacketed oil-saturated, (c) drained water-saturated, and (d) undrained water-saturated plane strain compression experiments.

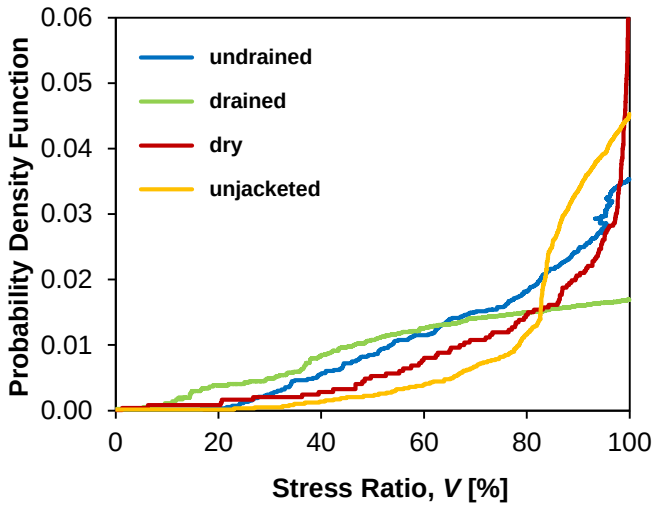

Fig. 3. Probability density function during dry (red), unjacketed (orange), drained (green), and undrained (blue) plane-strain compression experiments on fluid-saturated sandstone.

Presence of liquid water or some other reactive species in the crack tip environment can facilitate crack propagation by promoting weakening reactions, and this phenomenon is known as stress corrosion cracking (Atkinson and Rawlings, 1981; Atkinson, 1982). Increasing the pressure on a water-bearing environment enhances the rate of stress corrosions (Atkinson and Meredith, 1987; Heap et al., 2009) because the water molecules become more concentrated and chemical corrosion reactions increase. Not only does silicate-rich rock show AE during stress corrosion, but characteristics of AE can be related to mechanisms of fracture such as crack velocity, which makes AE an excellent instrument for monitoring the process (Baud et al., 2000).

The general observation is that the stress corrosion process starts at crack tips if the induced microcracks are connected to the porous network, as the transport of fluid is necessary. The observation that AE activity had initiated at significantly lower stress levels for water-saturated conditions comparing to dry and oil-saturated cases supports the assumption of the effect of chemically active fluid. Observed AE activity at low deviatoric stress and lower *RMS* value (associated with released energy) for the water-saturated specimen is believed to be associated with the stress corrosion cracking.

The findings of this study highlight the role of fluid type in laboratory experiments on induced seismicity. Working pore fluid should be chosen as close as possible to the in-situ fluid. If AE process and microseismisity in nature are qualitatively similar, the evaluations based on experimental results with a significant different type of fluid might overestimate or underestimate the onset of microseismic activity. For instance, if the injected fluid is chemically active, it might be expected that microseismic activity could be initiated at a lower stress level. In this case, microseismicity might not be an indication of stress state proximity to the critical conditions. On the other hand, if the injected fluid is inert, observation of the microseismicity might indicate a future earthquake.

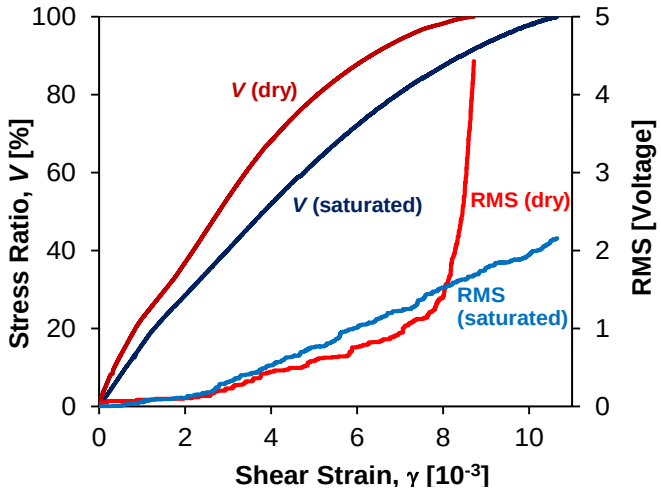

Fig. 4. Root-mean-square (RMS) value of AE energy and stress ratio function versus shear strain for dry and water-saturated drained plane strain compression experiments.

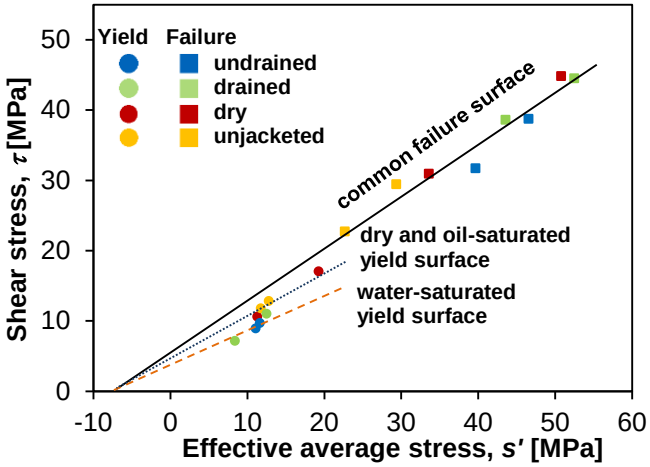

Fig. 5. Failure (squares) and yield (circles) point in $\tau - s'$ for dry (red), unjacketed (orange), drained(green), and undrained (blue) plane-strain compression experiments.

CONCLUSIONS

Analysis of acoustic emission (AE) was used for studying the effect of the pore fluid type on the microcracking activity. AE probability density functions were different for the specimens saturated with water and those saturated with oil or air (dry). Water-saturated specimens appeared to have a notably lower onset of inelasticity and the observed microcracking, initiated at low deviatoric stresses (25-30%), is explained by stress corrosion cracking. However, the total energy released by the AE was significantly larger closer to peak stress in dry rock compared to the water-saturated case, possibly due to the chemical weakening of the saturated specimen. Observed difference in AE behavior highlights the need in experiments with representative fluids for investigation of fluid-induced seismicity.

ACKNOWLEDGEMENTS

The authors acknowledge the support from US DOE through CarbonSAFE Macon County Project DE-FE0029381.

REFERENCES

Atkinson, B.K. 1982. Subcritical crack propagation in rocks: theory, experimental results and applications. *J. Struct. Geol.* 4(1): 41-56.

Atkinson, B.K., and P.G. Meredith. 1987. Experimental fracture mechanics data for rocks and minerals. In *Fracture Mechanics of Rock*, ed. B.K. Atkinson, Academic Press, London, 477-525.

Atkinson, B.K., and R.D. Rawlings. 1981. Acoustic emission during stress corrosion cracking in rocks. In *Earthquake Prediction – an International Review*, ed. D.W. Simpson, and P.G. Richards, AGU Maurice Ewing Series, 4: 605-616.

Baud, P., W. Zhu, and T.-f. Wong. 2000. Failure mode and weakening effect of water on sandstone. *J. Geophys. Res.* 105, B7: 16371-16389.

Benson, P.M., D.C. Austria, S. Gehne, E. Butcher, C.E. Harnett, M. Fazio, P. Rowley, and R. Tomas. 2020. Laboratory simulations of fluid-induced seismicity, hydraulic fracture, and fluid flow. *Geomech. Energy Environ.* 24: 100169.

Byerlee, J.D., and D. Lockner. 1977. Acoustic emission during fluid injection in rock. In *Proceedings, First conference on acoustic emission/microseismic activity in geological structures and materials*, eds. H.R. Hardy and Leighton F.W., 87-98. Clansthal-Zellerfeld: Trans Tech Publications.

Dai, S.T., and J.F. Labuz. 1997. Damage and failure analysis of brittle materials by acoustic emission. *J. Materials in Civ. Eng.* 9(4): 200-205.

Detournay, E and A.H.-D. Cheng. 1993. Fundamentals of poroelasticity. In *Comprehensive rock engineering*, ed. C. Fairhurst, 114-168.

Ellsworth, W.L. 2013. Injection-induced earthquakes. *Science*. 341(6142): 1225942.

Fischer, T., J. Horálek, P. Hrubcová, V. Vavryčuk, K. Bräuer, H. Kämpf. Intra-continental earthquake swarms in West-Bohemia and Vogtland: A review. *Tectonophysics*. 611: 1-27.

Heap, M.J., P. Baud, P.G. Meredith, A.F. Bell and I.G. Main. 2009. Time-dependent brittle creep in Darley Dale sandstone. *J. Geophys. Res.* 114: B07203.

Labuz, J.F., S.-T. Dai, and E. Papamichos. 1996. Plane-strain compression of rock-like material. *Int. J. Rock Mech. Min. Sci. & Geomech. Abstr.* 33(6): 573-584.

Lei, X., and S. Ma. 2014. Laboratory acoustic emission study for earthquake generation process. *Earthq. Sci.* 27(6): 627-646.

Li, X., X. Lei, and Q. Li. 2016. Injection-induced fracturing process in a tight sandstone under different saturation conditions. *Environ Earth Sci.* 75:1466.

Lockner, D. 1993. The role of acoustic emission in the study of rock. *Int. J. Rock. Mech. Min. Sci. & Geomech.* 30(7): 883-899.

Makhnenko, R.Y., C. Ge, and J.F. Labuz. 2020. Localization of deformation in fluid-saturated rock. *Int. J. Rock Mech. & Mining Sci.* 134, 104455

Makhnenko, R.Y., and J.F. Labuz. 2014. Plane strain testing with passive restraint. *Rock Mech. Rock Eng.* 47: 2021-2029.

Makhnenko, R.Y., and J.F. Labuz. 2016. Elastic and inelastic deformation of fluid-saturated rock. *Phil. Trans. R. Soc. A.* 374: 20150422.

Mayr, S.I., S. Stanchits, C. Langenbruch, G. Dresen, and S.A. Shapiro. 2011. Acoustic emission induced by pore-pressure changes in sandstone samples. *Geophysics* 76(3): MA21-MA31.

National Research Council. 2012. *Induced Seismicity Potential in Energy Technologies.* The National Academies Press, Washington, DC.

Ohtsu, M., K. Yuno, and Y. Inoue. 1993. Assessment of concrete deterioration by acoustic emission rate analysis. *J. Acoustic Emission* 11(4): S89-S98.

Rice, J.R. 1975. On the stability of dilatant hardening for saturated rock masses. *J. Geophys. Res.* 80(11): 1531–1536.

Scholz, C.H. 2019. *The mechanics of earthquakes and faulting*. 3rd ed. Cambridge: Cambridge University Press.

Smirnov, V.B., A.V. Ponomarev, A.V. Isaeva, N.B. Bondarenko, A.V. Patonin, P.A. Kaznacheev, S.M. Stroganova, M.G. Potanina, R. K. Chadha, and K. Arora. 2020. Fluid initiation of fracture in dry and water saturated rocks. *Izvestiya, Physics of the Solid Earth* 56: 808-826.

Sobolev, G.A., A.V. Ponomarev, Y.Y. Maibuk, N.A. Zakrzhevskaya, V.I. Ponyatovskaya, D.G. Sobolev, A.A. Khromov, and Y.V. Tsyvinskaya. 2010. The dynamics of the acoustic emission with water initiation. *Izvestiya, Physics of the Solid Earth* 46: 136-153.

Stanchits, S., S. Mayr, S. Shapiro, and G. Dresen. 2011. Fracturing of porous rock induced by fluid injection. *Tectonophysics* 503: 129-145.

Tarokh, A., R.Y. Makhnenko, K. Kim, X. Zhu, J.S. Popovics, B. Segvic, and D.E. Sweet. Influence of CO_2 on the poromechanical response of Berea sandstone. *Int. J. Greenh. Gas Con.* 95: 102959.

Zang, A., C.F. Wagner, and G. Dresen. 1996. Acoustic emission, microstructure, and damage model of dry and wet sandstones stressed to failure. *J. Geophys. Res.* 101: 17507-17521.